IEEE Access
Multidisciplinary | Rapid Review | Open Access Journal

Received October 16, 2018, accepted November 4, 2018, date of publication December 6, 2018,
date of current version December 31, 2018.

Digital Object Identifier 10.1109/ACCESS.2018.2885015

Simple Design Procedure of a Broadband Circularly Polarized Slot Monopole Antenna Assisted by Characteristic Mode Analysis

HUY HUNG TRAN[1,2], NGHIA NGUYEN-TRONG[3], (Member, IEEE), AND AMIN M. ABBOSH[3], (Senior Member, IEEE)

[1]Division of Computational Physics, Institute for Computational Science, Ton Duc Thang University, Ho Chi Minh City 70000, Vietnam
[2]Faculty of Electrical and Electronics Engineering, Ton Duc Thang University, Ho Chi Minh City 70000, Vietnam
[3]School of Information Technology and Electrical Engineering, University of Queensland, Brisbane, QLD 4072, Australia

Corresponding author: Huy Hung Tran (tranhuyhung@tdtu.edu.vn)

This work was supported by the Australian Research Council under Grant ARC LP160100917.

ABSTRACT In this paper, a systematic design procedure of a compact and broadband circularly polarized (CP) antenna is proposed. The antenna is first designed with a C-shaped monopole, and then a C-shaped slotted patch is utilized to produce CP radiation in the lower frequency band. Thus, the antenna's overall CP bandwidth (BW) is significantly increased. In addition, unlike the conventional method in which the operation is verified by the simulated surface current distribution, characteristic mode analysis (CMA) is carried out to give more insight into different modes on the antenna and generation of circular polarization. The CMA also helps to realize a structural optimization and identify an efficient feed location. The optimized antenna prototype with a compact size of $0.29\lambda_o \times 0.29\lambda_o \times 0.01\lambda_o$ (λ_o is the minimum wavelength at the minimum operation frequency) achieves a usable 10-dB reflection coefficient and 3-dB axial ratio fractional BW of 91% (2.1–5.6 GHz). The antenna realized broadside gain varies from 1.5 to 3.2 dBic within this measured overlapped BW.

INDEX TERMS UWB antenna, circularly polarized (CP), characteristic mode (CM), monopole, slot.

I. INTRODUCTION

In the era of modern wireless communications, there are extensive research activities into circularly polarized (CP) antennas with broadband characteristic for ultra-wideband (UWB) systems. They were able to be accomplished by various types of structures, i.e., dielectric resonators [1], [2], dipole antennas [3]–[5], or microstrip patches [6], [7]. However, due to the requirement of a ground plane reflector, these designs are featured by complicated structures, large overall dimensions and/or limited CP bandwidths (BWs).

For applications that do not require ground plane reflectors, the use of printed slot antennas [8]–[13], monopole [14]–[19] and dipole antennas [20], [21] have been investigated. These types of antennas were demonstrated to realize very wide operation bandwidth (BW) with low profile, low structural complexity as well as fabrication cost. Various antenna configurations have been reported with a wide range of different geometries, from basic shapes such as rectangle [19], [20], ellipse [14] to more irregular ones, e.g. U-shape [13], T-shape [18], C-shape [11], [16], [17]. However, the working principle is not clear since all of them depend on the simulated field distribution of the optimized design, which serves only as a verification tool rather than a design approach. Additionally, different shapes seem to be arbitrary choices, i.e. in a trial-and-error basis.

The characteristic mode analysis (CMA) has been proved to give the insightful physical understanding of the antenna's operating mechanism [22]–[25]. It provides the natural characteristics of electromagnetic resonance with current distribution and far field radiation pattern [26], [27]. This information can be used to evaluate the antenna's performance and useful in optimization process [28]–[38]. Utilizing CMA, this paper presents a methodical approach to design CP antenna for compact size and broadband operation. For higher band CP radiation, the proposed design employs a C-shaped monopole, which couples with a C-shaped slotted patch to extend the operating frequency into lower region.

The main focus of this paper is to provide a systematic and theoretical approach to design this type of antenna. As a validation, an antenna is optimized, fabricated and measured to demonstrate an UWB CP operation bandwidth of 91%, which is comparable to the state-of-the-arts designs. The antenna is analyzed and optimized using CST Microwave Studio commercial software. The proposed approach makes use of both CMA and numerical simulation tools, where CMA is only carried out for simple geometries for a very quick estimation on the structure parameters followed by the full-wave simulation, which is used to fine-tune the parameters. It is noted that for wideband antenna, the CMA takes significantly long time to completely track a large number of modes. Thus, the proposed approach is well-suited for this type of antenna.

II. CHARACTERISTIC MODE ANALYSIS FOR CP ANTENNAS

Characteristic modes (CM) are current modes obtained numerically for arbitrarily shaped conducting bodies. They are independent of any kind of excitation and only depend on the size and shape of the conducting object. The CM theory is extensively described in [22] and [23] for perfect electric conductor. It is extended for composite metal-dielectric structures in [24], in which the characteristic modes results are obtained by using a Method of Moments based on surface integral equation. For the design of the proposed CP antenna, only two important parameters, namely characteristic angle (α_n) and modal significance (MS_n) as the function of eigenvalue (λ_n), are required to be considered:

$$\alpha_n = 180^\circ - \tan^{-1}(\lambda_n) \quad (1)$$

$$MS_n = 1/|1 + j\lambda_n| \quad (2)$$

The characteristic angle models the phase difference between the characteristic current, J_n, and the associated characteristic field, E_n. The characteristic angle is defined and its physical meaning was discussed comprehensively in [25]. The mode is at resonance and becomes a good radiator when α is close to 180°. On the other hand, when α is near 90° or 270°, the mode mainly stores energy [23]. The modal significance is the normalized amplitude of the current mode and it represents the contribution of a particular mode to the total radiation when a source is applied.

To generate efficient CP radiation, two orthogonal modes should be excited simultaneously with 90° phase difference. Thus, the requirements for these two modes are:

1. The current distributions are orthogonal to each other,
2. The modal significances are the same $MS_1 = MS_2$,
3. The characteristic angles are $\alpha_1 = 135^\circ$ and $\alpha_2 = 225^\circ$, i.e. 45° difference from the resonance angle of 180°.
4. The directivities are the same at the angle of interest.

It should be noted that although a single mode of characteristic angles of 135° or 225° (corresponding to $\lambda_n = 1$ or -1) has low radiating efficiency due to high stored reactive energy, the combination of these two modes with same modal significance $MS_1 = MS_2$ can still yield 100% of radiation efficiency. This is because the extra inductive power in one mode compensates for the extra capacitive power in the other mode. The pair of modes with characteristic angles of 135° and 225° has been utilized to design CP antenna as shown in [23], [28], [34], and [35].

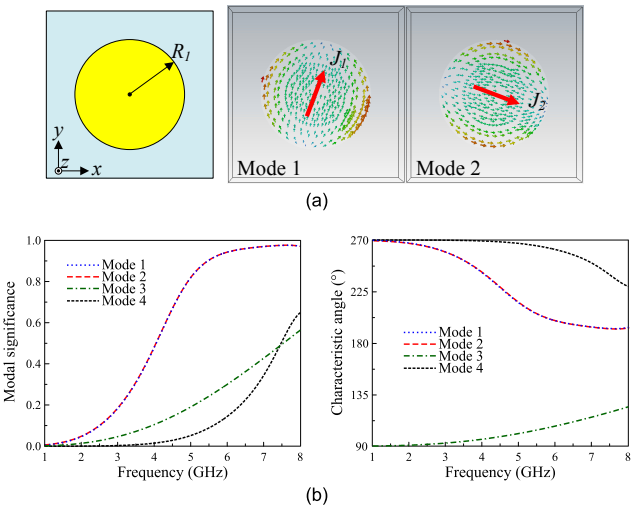

FIGURE 1. (a) Geometry and current distribution at 5.5 GHz for the first two modes and (b) Modal significance and characteristic angle of the circular patch antenna. The design parameter $R_1 = 11$ mm.

III. CP GENERATION PRINCIPLE

A. C-SHAPED MONOPOLE ANTENNA

For better demonstration of the design principle, the CMA is first carried out for a symmetric circular-shaped patch, which serves as an introduction towards the more complicated structure later. To note that there is currently no ground plane and the substrate (Taconic RF-35 with $\varepsilon_r = 3.5$ and thickness of 1.5 mm) is assumed to be loss-free and infinite in CMA. This patch becomes a monopole with the presence of a ground plane placed next to it [15]. The patch is designed to operate at around 5.5 GHz and the first 4 characteristic modes are calculated using numerical simulation software. Higher order modes have maximum modal significance at much higher frequencies. Fig. 1 shows the characteristic modes and characteristic current distribution of the circular patch. It can be seen that around 5.5 GHz, Mode 1 (J_1) and Mode 2 (J_2) are dominant and these two fundamental modes are featured by two perpendicular currents. However, their phase difference is 0° and hence, J_1 and J_2 cannot contribute to the CP realization.

To differentiate the characteristic angle between two orthogonal modes, the circular patch is modified such that the effective lengths in x- and y-direction are different. In this paper, we choose C-shaped patch, which is generated by subtracting a main circular patch from another eccentric circle (Fig. 2). It is noted that the use of other shapes such as U-shaped and ellipse shaped [13], [14] have the

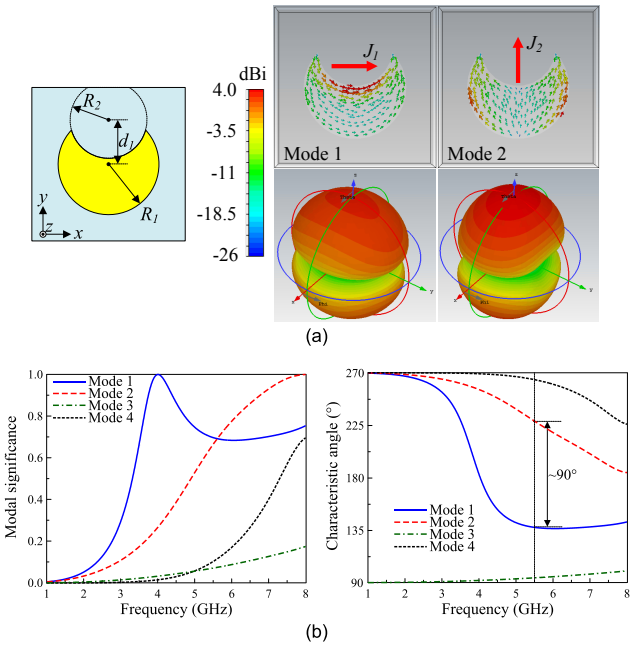

FIGURE 2. (a) Geometry, current distribution and far-field radiation at 5.5 GHz and (b) modal significance and characteristic angle of the C-shaped patch antenna. The design parameters: $R_1 = 11$, $R_2 = 8$, $d_1 = 8$ (unit: mm).

same principle. With this configuration, it obsevers the modes J_1 and J_2 are shifted away from each other. Fig. 2(b) confirms the CP radiation requirements mentioned in Section II: at around 5.5 GHz, the magnitudes of J_1 and J_2 are almost the same and they present a phase difference of 90°. In addition, their directivities at broadside direction are almost similar. Thus, if these two modes are properly excited and combined, they would yield CP radiation at this frequency band.

B. C-SHAPED SLOTTED PATCH ANTENNA

Next, a C-shaped slot is embedded in the center of a squared patch to realize CP operation at lower frequency band. Fig. 3 shows the geometry of the squared-patch with C-shaped slot aperture and its modal significance and characteristic angle of the first 5 modes. Typically, in a wide range of frequency, mode tracking can be an issue as can be seen in Fig. 3 with several unnatural transitions [39]. For this geometry, the first transition occurs at 4 GHz (mode 2 and mode 3). Thus, we limit discussion in the following to the frequency range up to 4 GHz, where a fast CMA can be run with a reasonable accuracy. For frequency higher than 4 GHz, better mode tracking and extra examination on electric field distribution should be performed.

For optimization of this design, the patch size, W_p, is not critical and should be chosen less than $0.5\lambda_L$ (λ_L is the effective wavelength at the lowest frequency) due to the fact that the slot will lower the resonance frequency of the structure. In this design, it is selected as $0.4\lambda_L$. Meanwhile, the dimensions of the slot (d_2, R_3, R_4) are more critical and they are optimized to provide satisfactory modal significane and characteristic angle reponses. Here, Mode 3 is ignored as

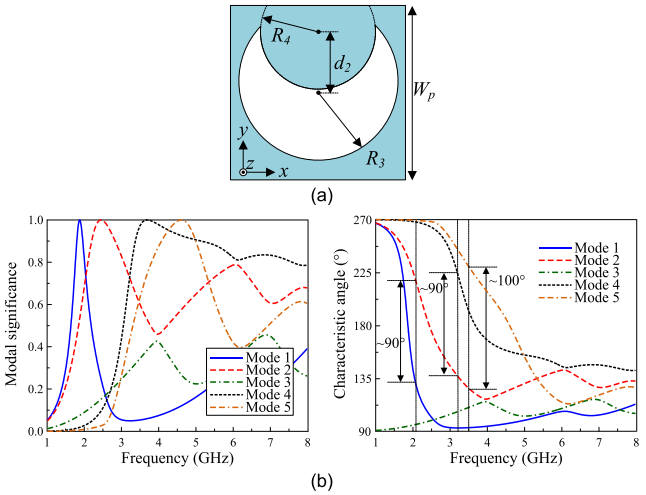

FIGURE 3. (a) Geometry and (b) Modal significance and characteristic angle of the C-shaped slotted patch antenna. The design parameters: $W_p = 42$, $R_3 = 18$, $R_4 = 13$, $d_2 = 13$ (unit: mm).

its resonance is at much higher frequency (the mode number is automatically sorted by CST at 2.1 GHz). It observes the similar phenomenon occurred at the two fundamental modes J_1 and J_2 of the C-shaped monopole and the C-shaped slot squared patch. These modes present the same current magnitude at 2.1 GHz. Additionally, it is found that the same modal significances are also obtained at higher frequencies of 3.2 and 3.5 GHz, which are the combination of the mode J_2 and higher-order modes J_4 and J_5. From the information provided by characteristic angle curves, the phase difference between their modes at these frequencies is quite close to 90°. However, to verify the CP behavior at these frequencies, the current distributions of the slotted antenna at 2.1, 3.2, and 3.5 GHz need to be checked and the simulated results are illustrated in Fig. 4. It can be seen that J_1 and J_2 are respectively dominant at two perpendicular directions and equal in radiated magnitude at broadside direction. Similar phenomenon can be observed at 3.5 GHz for modes J_2 and J_5. Despite of having about 90° phase difference, the current directions of modes J_2 and J_4 are identical. Nevertheless, the CMA shows that the C-shaped slotted patch antenna has potential to radiate CP waves at 2.1 and 3.5 GHz.

IV. ANTENNA DESIGN AND CHARACTERISTICS

According to the abovementioned CMA, this section shows a comprehensive design procedure to achieve a compact and broadband CP antenna with the combination of the C-shaped monopole and the C-shaped slotted patch antennas. The target BW is approximately from 2 to 6 GHz.

A. CIRCULARLY POLARIZED C-SHAPED MONOPOLE ANTENNA

First, the C-shaped monopole antenna with 50-Ω microstrip feeding line is designed (Fig. 5). It is fabricated on a 1.5 mm-thick Taconic RF-35 substrate. The patch and ground plane are printed at two opposite sides of the substrate. CMA is

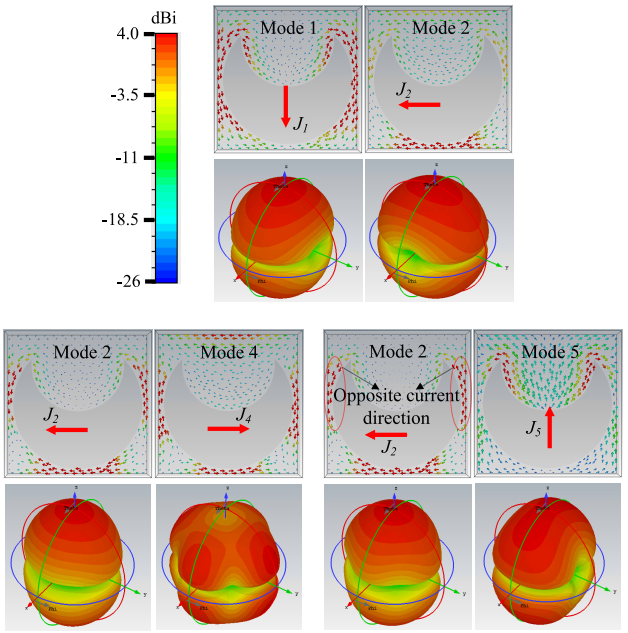

FIGURE 4. Simulated current distributions at (a) 2.1 GHz, (b) 3.2 GHz, and (c) 3.5 GHz. For Mode 2 and Mode 4, the currents in the vertical directions are opposite at two sides thus they cancel each other at broadside direction, leaving the dominant being the horizontal current J_2 and J_4 in horizontal direction.

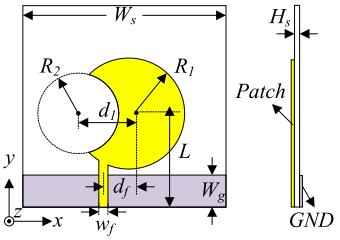

FIGURE 5. Geometry of the CP C-shaped monopole antenna. The design parameters: $R_1 = 11$, $R_2 = 8$, $d_1 = 10$, $L = 18$, $d_f = 5$, $w_f = 1.8$, $W_g = 5$, $W_s = 42$ (unit: mm).

performed to obtain initial design parameters as shown in Section II.A. It is noted that the CMA, typically around 20s for this structure, is significantly faster than running a full-wave simulation. The antenna is optimized to work at frequency range around 5 GHz, i.e. the upper range of the target operating BW, and the final dimensions of the designed antenna are shown in the caption of Fig. 5.

Based on the current distribution shown in Fig. 2(b), we can identify where the feed point should be located to excite the orthogonal modes, J_1 and J_2. The principle is to feed the antenna where the two modes are excited with the same magnitude [27]. This can be done by subtracting J_1 from J_2 and identifying the position with minimum difference value. It is found that the optimal feed locations are at the corner of the C-shaped patch. To verify this, Fig. 6 presents the simulated $|S_{11}|$ and AR for different positions of feed line. By simply moving the feed position from the center to the corner of the patch, the impedance matching and AR BWs

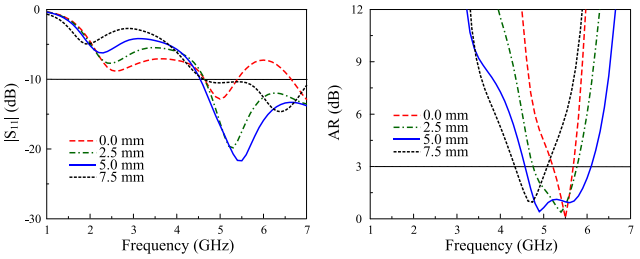

FIGURE 6. Simulated (a) $|S_{11}|$ and (b) AR of the C-shaped monopole antenna with different positions of feed line, d_f.

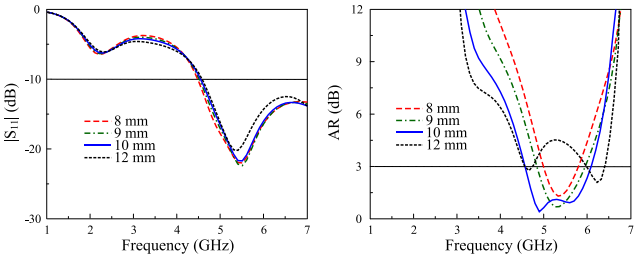

FIGURE 7. Simulated (a) $|S_{11}|$ and (b) AR of the C-shaped monopole antenna with different positions of subtracted circle, d_1.

are improved with the best performance when $d_f = 5$ mm. Next, the position of the eccentric circular, d_1, is investigated and the antenna performances against the variation d_1 are depicted in Fig. 7. It observes a minor change in the impedance BW, while the effects of d_1 on AR BW is more pronounced. Nevertheless, with the key antenna dimensions and feeding position obtained from CMA, the antenna performance is quite immune to parameter variations. With this type of feeding, the C-shaped monopole is able to achieve the best usable fraction BW of 28%, ranging from 4.6 to 6.1 GHz. This simulated result agrees well with the CMA of the C-shaped patch demonstrated in Section III.A.

B. CIRCULARLY POLARIZED C-SHAPED MONOPOLE AND C-SHAPED SLOTTED PATCH ANTENNA

As discussed earlier, to improve the CP BW, a C-shaped slotted patch is employed to operate at the lower frequency band. Fig. 8 shows the configuration of the final design CP antenna.

To optimize this antenna, CMA is first used to obtain the initial parameters of the squared patch and the slot as shown in Section III.B, i.e. with the potential CP resonances at the lower range (2.1 and 3.5 GHz) of the target BW. This slotted patch is then fed by the C-shaped monopole optimized in Section IV.B. The slotted patch is excited through a coupling mechanisim with the directed fed C-shaped monopole. Therefore, the position of the monopole plays an important role on the performance of the slotted patch. Here, by using CMA again, we can also predict the satisfactory location of the C-shaped monopole, which is located closely to the edge of the slot to excite the required modes (J_1, J_2, J_5) for CP

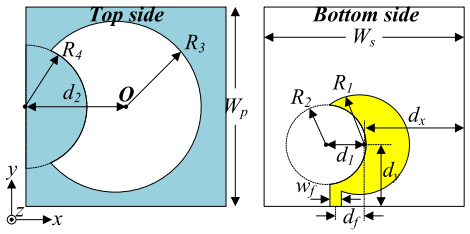

FIGURE 8. Geometry of the broadband C-shaped monopole and slot antenna. The design parameters: $R_3 = 18$, $R_4 = 13$, $d_2 = 19$, $R_1 = 11$, $R_2 = 8.4$, $d_1 = 7$, $d_x = 22$, $d_y = 12.5$, $d_f = 6$, $w_f = 2.4$, $W_s = 42$ (unit: mm).

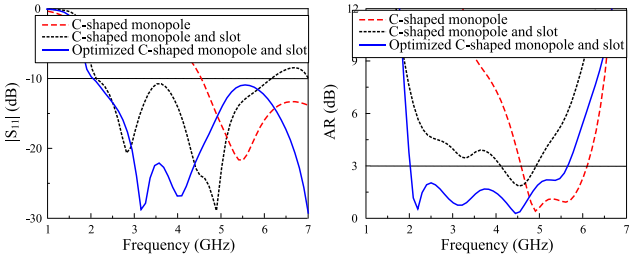

FIGURE 9. Simulated (a) $|S_{11}|$ and (b) AR of the C-shaped monopole antenna with and without C-shaped slot.

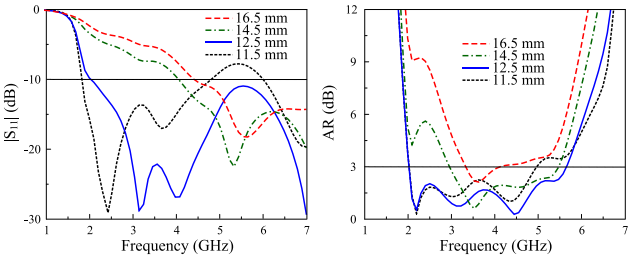

FIGURE 10. Simulated (a) $|S_{11}|$ and (b) AR of the C-shaped monopole and the C-shaped slotted patch antenna for different position of the monopole along y-axis, d_y.

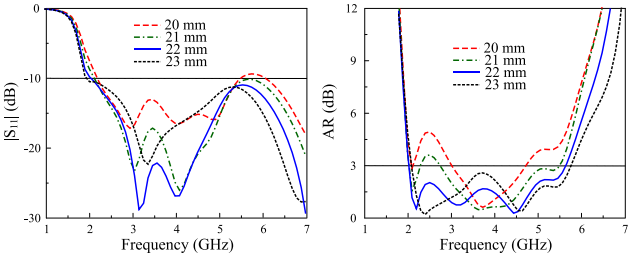

FIGURE 11. Simulated (a) $|S_{11}|$ and (b) AR of the C-shaped monopole and the C-shaped slotted patch antenna for different position of the monopole along x-axis, d_x.

radiation at 2.1 and 3.5 GHz. This is similar to the feeding of the C-shaped monopole.

It should be clarified here that a CMA for the final design (Fig. 8) across a wide bandwidth (2 to 6 GHz) is time-consuming, with difficulty in mode tracking, thus it is not used for the optimization here. However, for the proposed design, since the CP monopole is fed directly, it is reasonable to expect that the modes associated with the monopole are dominant around 5 GHz. Furthermore, since the monopole does not radiate at low frequency, the low-frequency operation is dominant by the C-shaped slotted patch. The dotted black curve in Fig. 9 shows the performance of the antenna with the dimensions obtained from the CMA in Section III and IV.A. As expected, a potential wideband performance can be achieved. The design is then fine-tuned using numerical full-wave simulation software and the optimized results are shown as solid blue curve in Fig. 9. The results show that a very wide CP BW of 96.1% can be achieved in this configuration. For readers' convenience, we show some key parameter studies in the following, noting that only one parameter is varied while the others are kept as their optimized values shown in Fig. 8's caption. Fig. 10 shows the simulated $|S_{11}|$ and AR results when moving the monopole along y-axis, d_y. As decreasing d_y, the monopole will be more close to the edge of the slot and therefore the impedance matching and AR can be significantly improved. The AR can be further improved by slightly tuned the position of the monopole along x-axis, d_x, as shown in Fig. 11. These results agree well with the prediction based on the CMA about the position of the monopole, which is critical to determine the overall operating BW of the antenna. In addition, according to the information provided in Figs. 6 and 7, the impedance matching and AR in the upper band can be adjusted by tuning d_1 and d_f. In contrast, the CP radiation in lower band can be optimized by properly tuning d_2 and R_4, which is expected as the C-shaped slot controls the lower frequency performance. For brevity, Fig. 12 only presents the effect of d_2 on the antenna reflection coefficient and AR.

C. DESIGN PROCEDURE

The design procedure can summarized as:

Step 1: Use the theory of CM to predict the initial values for the C-shaped monopole (R_1, R_2, d_1) and the C-shaped slotted patch (W_p, R_3, R_4, d_2) to achieve CP radiation at desired frequency bands (W_p is not critical for CP performance). Based on the simulated characteristic currents, predict the optimal feeding positions.

Step 2: Design the CP C-shaped monopole antenna with ground plane and feeding line. Tune d_f, w_f to obtain satisfactory S_{11} performance. The CP operation is optimized by tuning R_2 and d_1.

Step 3: Replace the ground plane with the C-shaped slotted patch. Adjust the position of the monopole by simply tuning d_x, d_y to achieve reasonable overall S_{11} and AR performances.

Step 4: Final tune R_2, d_1 to achieve the best performance in upper band and R_3, d_2 for lower band.

V. MEASUREMENT RESULTS

A prototype of the proposed antenna has been fabricated and tested. The photograph of the fabricated antenna is shown in Fig. 13. Fig.s 14 and 15 depict the antenna's simulated

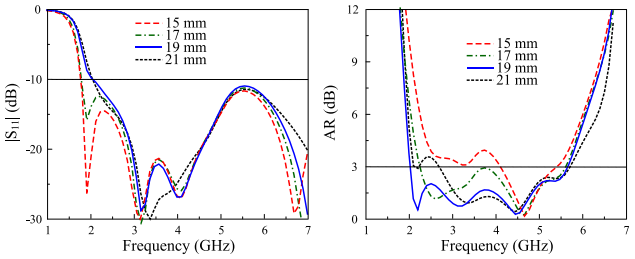

FIGURE 12. Simulated (a) $|S_{11}|$ and (b) AR of the C-shaped monopole and the C-shaped slotted patch antenna for different values of d_2.

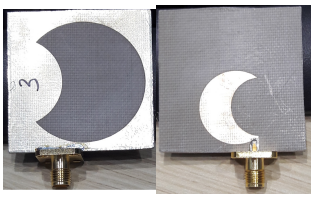

FIGURE 13. Fabricated antenna.

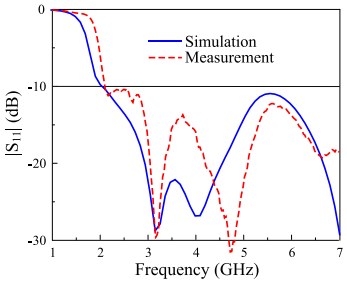

FIGURE 14. Simulated and measured $|S_{11}|$.

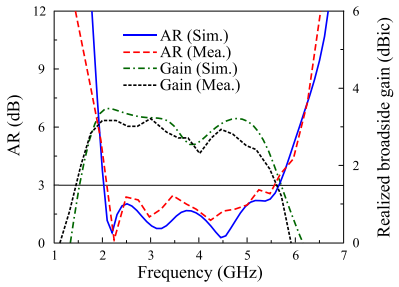

FIGURE 15. Simulated and measured AR and realized gain.

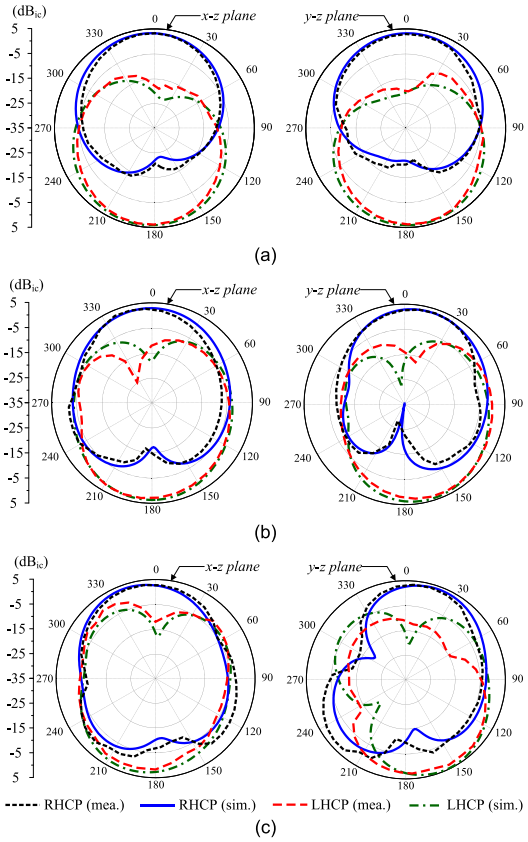

FIGURE 16. Simulated and measured realized gain radiation patterns at (a) 3 GHz, (b) 4 GHz, and (c) 5 GHz.

TABLE 1. Performance Comparison Among CP Antennas Using Monopole and/or Slot Structures.

Ref.	Lateral size (λ_o)	Operation BW (%)	Realized gain (dBic)
[11]	0.40 × 0.40	96	4.7
[13]	0.29 × 0.29	110	4.5
[14]	0.44 × 0.37	84	3.4
[16]	0.37 × 0.33	98	6.4
[19]	0.18 × 0.18	129	3.5
[21]	0.74 × 0.49	97	4.5
Prop.	**0.29 × 0.29**	**91**	**3.2**

and measured results in terms of reflection coefficient, AR, and realized broadside gain. A good agreement between simulation and measurement is observed. The antenna is able to achieve good performance in the wide range of frequency band from 2.1 to 5.6 GHz, equivalent to 91% fractional BW. Additionally, the measure realized broadside gain within this usable BW is varied from 1.5 to 3.2 dBic.

The simulated and measured radiation patterns at different frequencies in two principle planes are plotted in Fig. 16. The antenna exhibits bi-directional radiation characteristics with right-hand CP (RHCP) in the $+z$ direction and left-hand CP (LHCP) in the $-z$ direction. Furthermore, the isolations between RHCP and LHCP radiations for both $\pm z$ directions are always better than 15 dB entire the usable BW.

Finally, we present the performance comparison between the proposed antenna and the other report CP antennas using monopole and/or slot structures in Table 1. Overall, the antenna shows a comparable performance with state-of-the-art designs. Apparently, there is a trade-off among lateral sizes, CP operation BW and maximum gain. Although the designs in [13] and [21] show a wider BW, their reported radiation patterns were tilted to be quite off broadside while the main beam in the proposed design tends to remain at broadside across the frequency range (Fig. 16). Nevertheless, the proposed technique has its value in giving more insightful into the working principle as well as providing a

comprehensive design guideline with a well-defined geometry. Using the proposed approach, some broadband antennas in recent literature can be revisited with the CM as a complement analysis.

VI. CONCLUSION

This paper demonstrated a compact and broadband CP antenna using the combined monopole and slot structures. A systematic design procedure is proposed with the aid of the theory of CM. The antenna has been designed and well understood with established electromagnetic principles. The present findings can inspire the study of different of antennas using CM to give more theoretical insights and possibly more efficient optimization process. A final antenna with overall size of $0.29\lambda_o \times 0.29\lambda_o \times 0.01\lambda_o$, where λ_o is the wavelength at the lowest operation frequency, yields usable fractional BW for $|S_{11}| \leq -10$ dB and AR ≤ 3 dB of 91%, ranging from 2.1 to 5.6 GHz. The antenna has bi-directional radiation pattern and measured gain of from 1.5 to 3.2 dBic within the usable BW.

REFERENCES

[1] L. Lu, Y.-C. Jiao, H. Zhang, R. Wang, and T. Li, "Wideband circularly polarized antenna with stair-shaped dielectric resonator and open-ended slot ground," *IEEE Antennas Wireless Propag. Lett.*, vol. 15, pp. 1755–1758, 2016.

[2] G. Varshney, V. S. Pandey, R. S. Yaduvanshi, and L. Kumar, "Wide band circularly polarized dielectric resonator antenna with stair-shaped slot excitation," *IEEE Trans. Antennas Propag.*, vol. 65, no. 3, pp. 1380–1383, Mar. 2017.

[3] H. H. Tran, I. Park, and T. K. Nguyen, "Circularly polarized bandwidth-enhanced crossed dipole antenna with a simple single parasitic element," *IEEE Antennas Wireless Propag. Lett.*, vol. 16, pp. 1776–1779, 2017.

[4] W. J. Yang, Y. M. Pan, and S. Y. Zheng, "A low-profile wideband circularly polarized crossed-dipole antenna with wide axial-ratio and gain beamwidths," *IEEE Trans. Antennas Propag.*, vol. 66, no. 7, pp. 3346–3353, Jul. 2018.

[5] K. Kang, Y. Shi, and C.-H. Liang, "A wideband circularly polarized magnetoelectric dipole antenna," *IEEE Antennas Wireless Propag. Lett.*, vol. 16, pp. 1647–1650, 2017.

[6] J. Wei, X. Jiang, and L. Peng, "Ultrawideband and high-gain circularly polarized antenna with double-Y-shape slot," *IEEE Antennas Wireless Propag. Lett.*, vol. 16, pp. 1508–1511, 2017.

[7] K. Ding, C. Gao, T. Yu, D. Qu, and B. Zhang, "Gain-improved broadband circularly polarized antenna array with parasitic patches," *IEEE Antennas Wireless Propag. Lett.*, vol. 16, pp. 1468–1471, 2016.

[8] R. K. Saini and S. Dwari, "A broadband dual circularly polarized square slot antenna," *IEEE Trans. Antennas Propag.*, vol. 64, no. 1, pp. 290–294, Jan. 2016.

[9] M. S. Ellis, Z. Zhao, J. Wu, X. Ding, Z. Nie, and Q.-H. Liu, "A novel simple and compact microstrip-fed circularly polarized wide slot antenna with wide axial ratio bandwidth for C-band applications," *IEEE Trans. Antennas Propag.*, vol. 64, no. 4, pp. 1552–1555, Apr. 2016.

[10] T. T. Le, V. H. The, and H. C. Park, "Simple and compact slot-patch antenna with broadband circularly polarized radiation," *Microw. Opt. Technol. Lett.*, vol. 58, no. 7, pp. 1634–1641, Jul. 2016.

[11] R. Xu, J.-Y. Li, and J. Liu, "A design of broadband circularly polarized C-shaped slot antenna with sword-shaped radiator and its array for L/S-band applications," *IEEE Access*, vol. 6, pp. 5891–5896, 2017.

[12] T. T. Le, H. H. Tran, and H. C. Park, "Simple-structured dual-slot broadband circularly polarized antenna," *IEEE Antennas Wireless Propag. Lett.*, vol. 17, no. 3, pp. 476–479, Mar. 2018.

[13] R. Xu, J.-Y. Li, J.-J. Yang, K. Wei, and Y.-X. Qi, "A design of U-shaped slot antenna with broadband dual circularly polarized radiation," *IEEE Trans. Antennas Propag.*, vol. 65, no. 6, pp. 3217–3220, Jun. 2017.

[14] T. Fujimoto, T. Ishikubo, and M. Takamura, "A wideband printed elliptical monopole antenna for circular polarization," *IEICE Trans. Commun.*, vol. E100-B, no. 2, pp. 203–210, Feb. 2017.

[15] K. Ding, C. Gao, T. Yu, and D. Qu, "Broadband C-shaped circularly polarized monopole antenna," *IEEE Trans. Antennas Propag.*, vol. 63, no. 2, pp. 785–790, Feb. 2015.

[16] H. Tang, K. Wang, R. Wu, C. Yu, J. Zhang, and X. Wang, "A novel broadband circularly polarized monopole antenna based on C-shaped radiator," *IEEE Antennas Wireless Propag. Lett.*, vol. 16, pp. 964–967, 2017.

[17] K. Ding, C. Gao, Y. Wu, D. Qu, and B. Zhang, "A broadband circularly polarized printed monopole antenna with parasitic strips," *IEEE Antennas Wireless Propag. Lett.*, vol. 16, pp. 2509–2512, 2017.

[18] K. O. Gyasi *et al.*, "A compact broadband cross-shaped circularly polarized planar monopole antenna with a ground plane extension," *IEEE Antennas Wireless Propag. Lett.*, vol. 17, no. 2, pp. 335–338, Feb. 2018.

[19] D. S. Chandu and S. S. Karthikeyan, "Broadband circularly polarized printed monopole antenna with protruded L-shaped and inverted L-shaped strips," *Microw. Opt. Technol. Lett.*, vol. 60, no. 1, pp. 242–248, Jan. 2018.

[20] K. G. Thomas and G. Praveen, "A novel wideband circularly polarized printed antenna," *IEEE Trans. Antennas Propag.*, vol. 60, no. 12, pp. 5564–5570, Dec. 2012.

[21] R. Xu, J.-Y. Li, K. Wei, and G.-W. Yang, "Broadband rotational symmetry circularly polarized antenna," *Electron. Lett.*, vol. 52, no. 6, pp. 414–416, Mar. 2016.

[22] R. F. Harrington and J. R. Mautz, "Theory of characteristic modes for conducting bodies," *IEEE Trans. Antennas Propag.*, vol. 19, no. 5, pp. 622–628, Sep. 1971.

[23] M. Cabedo-Fabres, E. Antonino-Daviu, A. Valero-Nogueira, and M. F. Bataller, "The theory of characteristic modes revisited: A contribution to the design of antennas for modern applications," *IEEE Antennas Propag. Mag.*, vol. 49, no. 5, pp. 52–68, Oct. 2007.

[24] R. T. Maximidis, C. L. Zekios, T. N. Kaifas, E. E. Vafiadis, and A. G. Kyriacou, "Characteristic mode analysis of composite metaldielectric structure, based on surface integral equation/moment method," in *Proc. IEEE Eur. Conf. Antennas Propag. (EuCAP)*, Hague, The Netherlands, Apr. 2014, pp. 2822–2826.

[25] R. Garbacz and R. Turpin, "A generalized expansion for radiated and scattered fields," *IEEE Trans. Antennas Propag.*, vol. AP-19, no. 3, pp. 348–358, May 1971.

[26] S. Huang, J. Pan, and Y. Luo, "Study on the relationships between eigenmodes, natural modes, and characteristic modes of perfectly electric conducting bodies," *Int. J. Antennas Propag.*, vol. 2018, Apr. 2018, Art. no. 8735635.

[27] Y. Chen and C.-F. Wang, "Electrically small UAV antenna design using characteristic modes," *IEEE Trans. Antennas Propag.*, vol. 62, no. 2, pp. 535–545, Feb. 2014.

[28] Y. Chen and C.-F. Wang, "Characteristic-mode-based improvement of circularly polarized U-slot and E-shaped patch antennas," *IEEE Antennas Wireless Propag. Lett.*, vol. 11, pp. 1474–1477, 2012.

[29] M. Khan and D. Chatterjee, "Characteristic mode analysis of a class of empirical design techniques for probe-fed, U-slot microstrip patch antennas," *IEEE Trans. Antennas Propag.*, vol. 64, no. 7, pp. 2758–2770, Jul. 2016.

[30] F. H. Lin and Z. N. Chen, "Low-profile wideband metasurface antennas using characteristic mode analysis," *IEEE Trans. Antennas Propag.*, vol. 65, no. 4, pp. 1706–1713, Apr. 2017.

[31] J.-F. Lin and Q.-X. Chu, "Extending bandwidth of antennas with coupling theory for characteristic modes," *IEEE Access*, vol. 5, pp. 22262–22271, Oct. 2017.

[32] J.-F. Lin and Q.-X. Chu, "Increasing bandwidth of slot antennas with combined characteristic modes," *IEEE Trans. Antennas Propag.*, vol. 66, no. 6, pp. 3148–3153, Jun. 2018.

[33] J. Yang, J. Li, and S. Zhou, "Study of antenna position on vehicle by using characteristic modes theory," *IEEE Antennas Wireless Propag. Lett.*, vol. 17, no. 7, pp. 1132–1135, Jul. 2018.

[34] C. Zhao and C.-F. Wang, "Characteristic mode design of wide band circularly polarized patch antenna consisting of H-shaped unit cells," *IEEE Access*, vol. 6, pp. 25292–25299, 2018.

[35] K. Saraswat and A. R. Harish, "Analysis of wideband circularly polarized ring slot antenna using characteristics mode for bandwidth enhancement," *Int. J. RF. Microw. Comput. Aided Eng.*, vol. 28, no. 2, p. e21186, Feb. 2018.

[36] J. Zhao, Y. Chen, and S. Yang, "In-band radar cross-section reduction of slot antenna using characteristic modes," *IEEE Antennas Wireless Propag. Lett.*, vol. 17, no. 7, pp. 1166–1170, Jul. 2018.

[37] N. M. Mohamed-Hicho, E. Antonino-Daviu, M. Cabedo-Fabrés, and M. Ferrando-Bataller, "Designing slot antennas in finite platforms using characteristic Modes," *IEEE Access*, vol. 6, pp. 41346–41355, Jun. 2018.
[38] E. Antonino-Daviu, M. Cabedo-Fabrés, M. Sonkki, N. M. Mohamed-Hicho, and M. Ferrando-Bataller, "Design guidelines for the excitation of characteristic modes in slotted planar structures," *IEEE Trans. Antennas Propag.*, vol. 64, no. 12, pp. 5020–5029, Dec. 2016.
[39] B. D. Raines and R. G. Rojas, "Wideband characteristic mode tracking," *IEEE Trans. Antennas Propag.*, vol. 60, no. 7, pp. 3537–3541, Jul. 2012.

HUY HUNG TRAN received the B.S. degree in electronics and telecommunications from the Hanoi University of Science and Technology, Hanoi, Vietnam, in 2013, and the M.S. degree in electrical engineering from Ajou University, Suwon, South Korea, in 2015. He is currently a Researcher with the Institute of Computational Science, Ton Duc Thang University, Ho Chi Minh City, Vietnam.

His current research interests include circularly polarized antennas, high gain antennas, metamaterial-based antennas, and reconfigurable antennas.

NGHIA NGUYEN-TRONG (S'12–M'17) received the Ph.D. degree in electrical engineering from The University of Adelaide, SA, Australia, in 2017. He is currently a Post-Doctoral Research Fellow with The University of Queensland, QLD, Australia.

His current research interests include leaky-wave antennas, monopolar antennas, Fabry–Perot antennas, and reconfigurable antennas. He was one of the recipients of the Best Student Paper Award at the 2014 IWAT, the 2015 IEEE MTT-S NEMO, and the 2017 ASA conferences, and the Best Paper Award at the 2018 AMS Conference. He was selected as a Top Reviewer of the IEEE TRANSACTIONS ON ANTENNAS AND PROPAGATION and the IEEE ANTENNAS AND WIRELESS PROPAGATION LETTERS, in 2018.

AMIN M. ABBOSH (SM'08) received the Dr. Eng. degree from The University of Queensland, in 2013. He currently leads the Microwave Group, The University of Queensland, Australia, where he is also the Director of research with the School of ITEE. He has authored more than 400 papers on electromagnetic imaging systems for medical applications, wideband passive microwave devices, and planar antennas. His co-authored paper Optimization-Based Confocal Microwave Imaging in Medical Applications, IEEE-TAP, 63-8, received the IEEE APS King Award for the best paper published in 2015. He is an Associate Editor of the IEEE TRANSACTIONS ON ANTENNAS AND PROPAGATION and the IEEE ANTENNAS AND WIRELESS PROPAGATION LETTERS.